Magnetic Resonance and Fluorescence–Protein Imaging of the Anti-angiogenic and Anti-tumor Efficacy of Selenium in an Orthotopic Model of Human Colon Cancer

ARUP BHATTACHARYA[1], STEVEN G. TUROWSKI[2], IVAN DOMINGUEZ SAN MARTIN[3], ASHWANI RAJPUT[4], YOUCEF M. RUSTUM[5], ROBERT M. HOFFMAN[6,7] and MUKUND SESHADRI[2]

Departments of [1]Cancer Prevention and Control, [2]Pharmacology and Therapeutics, [3]Surgical Oncology, Roswell Park Cancer Institute, Elm and Carlton Streets, Buffalo, NY, U.S.A.; [4]Department of Surgery, Division of Surgical Oncology, University of New Mexico, Albuquerque, NM, U.S.A.; [5]Department of Cancer Biology, Roswell Park Cancer Institute, Buffalo, NY, U.S.A.; [6]AntiCancer Inc., San Diego, CA, U.S.A.; [7]Department of Surgery, University of California, San Diego, CA, U.S.A.

Abstract. *Tumor progression and angiogenesis are intimately related. To understand the interrelationship between these two processes, real-time imaging can make a major contribution. In this report, fluorescent protein imaging (FPI) and magnetic resonance imaging (MRI) were utilized to demonstrate the effects of selenium on tumor progression and angiogenesis in an orthotopic model of human colon cancer. GEO (well-differentiated human colon carcinoma), cells transfected with green fluorescent protein (GFP), were implanted orthotopically into the colon of athymic nude mice. Beginning five days post implantation, whole-body FPI was performed to monitor tumor growth in vivo. Upon successful visualization of tumor growth by FPI, animals were randomly assigned to either a control group or a treatment group. Treatment consisted of daily oral administration of the organoselenium compound, methyl-selenocysteine (MSC; 0.2 mg/day × five weeks). Dynamic contrast-enhanced MRI was performed to examine the change in tumor blood volume following treatment. CD31 immuno-staining of tumor sections was also performed to quantify microvessel density (MVD). While T1- and T2-weighted MRI provided adequate contrast and volumetric assessment of GEO tumor growth, GFP imaging allowed for high-throughput visualization of tumor progression in vivo. Selenium treatment resulted in a significant reduction in blood volume and microvessel density of GEO tumors. A significant inhibition of tumor growth was also observed in selenium-treated animals compared to untreated control animals. Together, these results highlight the usefulness of multimodal imaging approaches to demonstrate antitumor and anti-angiogenesis efficacy and the potential of selenium treatment of colon cancer.*

The development of targeted therapies for cancer in recent years has been accompanied by parallel advances in imaging technologies to enable assessment of their efficacy. In preclinical model systems, several imaging modalities including magnetic resonance imaging (MRI), computed tomography (CT), positron-emission tomography (PET) and optical imaging methods have been utilized to evaluate the pharmacologic activity of novel targeted therapies (1-3). However, each of these imaging methods has distinguishable advantages and limitations as well as marked differences in their sensitivity of detection, and spatial and temporal resolution. The use of multiple imaging methods is therefore likely to provide complimentary information on tumor biology.

Studies have previously examined the use of optical imaging techniques such as fluorescent protein imaging (FPI) and bioluminescence imaging in combination with clinical imaging methods such as MRI and PET (4-6). Bouvet *et al.* previously demonstrated a high degree of correlation between FPI and MRI in an orthotopic model of pancreatic cancer (6). Recently, Gros *et al.* demonstrated the utility of combining MRI and FPI in an orthotopic model of esophageal cancer (7). However, the majority of these reports primarily examined anatomic correlation between multiple imaging techniques. In this study, a combined dual-modality

Correspondence to: Mukund Seshadri, DDS, Ph.D., Department of Pharmacology and Therapeutics, Roswell Park Cancer Institute, Elm and Carlton Streets, Buffalo, NY 14263, USA. Tel: +1 7168451552, Fax: +1 7168451764, e-mail: mukund.seshadri@roswell_park.org

Key Words: Colon cancer, orthotopic model, GFP, fluorescent protein imaging (FPI), MRI, selenium, angiogenesis.

imaging approach was utilized to characterize changes in tumor growth and vascular function in an orthotopic human colon adenocarcinoma nude-mouse model following treatment with the organoselenium compound, methylselenocysteine (MSC). Previous studies have demonstrated the antiangiogenic and antitumor activity of selenium compounds in ectopic models of human cancer (8, 9). However, the activity of selenium on tumor angiogenesis and growth of orthotopic human tumors has not been extensively studied. Therefore, the effects of selenium in the orthotopic GEO human colon adenocarcinoma were examined. FPI- and MRI-based measures of tumor growth and vascular response to treatment were correlated with immunohistochemical estimates of microvessel density (MVD). Long-term response to selenium treatment was assessed by monitoring tumor growth over a 60-day period.

Materials and Methods

Animals. Eight-to-twelve-week-old female athymic nude mice (*nu/nu*, body weight, 20-25 g) were obtained from Harlan Sprague Dawley, Inc. (Indianapolis, IN, USA) and housed in microisolator cages (four to five animals per cage). Animals were provided with food and water *ad libitum* and maintained on 12-hour light/dark cycles in a HEPA-filtered environment within the Laboratory Animal Resource at Roswell Park Cancer Institute.

Surgical procedure for orthotopic implantation. GEO human cancer cells were labeled with green fluorescent protein (GFP) using a retroviral transfection technique described previously (10). Subcutaneous tumors were initially established in donor mice by injection of 5×10^6 GEO cells under isoflurane anesthesia (Abbott Laboratories, Abbott Park, IL, USA). Upon successful establishment of tumors (~500 mm^3) from the cell lines for at least two passages, tumors were harvested and cut into smaller fragments (~1 mm/20 mg) for surgical orthotopic implantation into recipient mice. Under transient isoflurane anesthesia, a 1 cm laparotomy was performed and two individual pieces of tumor tissue were subserosally implanted into the cecum and ascending colon using an aseptic technique (10-12). Surgical procedures were performed in accordance with protocols approved by the Institutional Animal Care and Use committee at Roswell Park Cancer Institute.

Fluorescence imaging. Fluorescence imaging was performed periodically to monitor tumor growth and progression *in vivo*. Images were obtained using a fluorescence imaging system (Light Box; Light Tools Research, Encinitas, CA, USA) equipped with a fiber optic illumination at 470 nm. Images were collected through a 515 nm long-pass filter and captured using Imaging software (Burnaby, British Columbia, Canada). Images were optimized for contrast and brightness using commercial software (Adobe Photoshop, CS2; Adobe, San Jose, CA, USA).

Drug treatment. MSC was obtained from Sigma (St. Louis, MO, USA) and dissolved in sterile saline at a concentration of 1 mg/ml. For studies, MSC was administered orally at a dose of 0.2 mg/mouse/day beginning 6 days after tumor implantation.

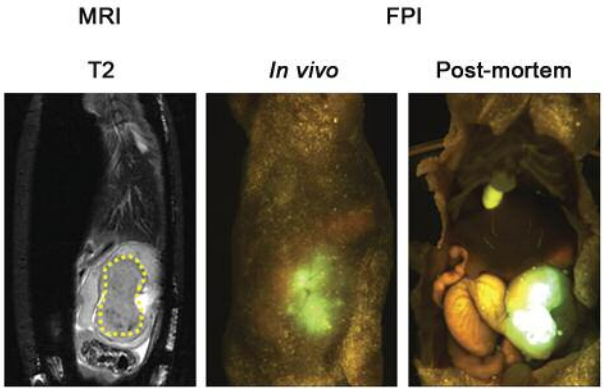

Figure 1. *Combined magnetic resonance imaging (MRI) and green fluorescent protein imaging (FPI) in an orthotopic model of human colon cancer. A single slice from coronal T2-weighted MR image of a nude mouse bearing a GEO colon tumor (outlined in yellow) is shown on the left. Corresponding live and postmortem FPI images of the same animal are shown on the right.*

Magnetic resonance imaging. MRI studies were performed using a 4.7-T/33-cm horizontal bore magnet (GE NMR Instruments, Fremont, CA, USA) incorporating AVANCE digital electronics (Bruker Biospec, ParaVision 3.0.2 (OS); Bruker Medical, Billerica, MA, USA). Induction of anesthesia prior to imaging and maintenance of anesthesia during imaging was achieved by inhalation of isoflurane (~2-3% in oxygen). Anesthetized animals were placed on an acrylic sled for positioning within the magnet bore. Monitoring of the body temperature and physiological parameters during imaging was accomplished using an air heater system in conjunction with respiratory and temperature sensors located within the sled. Preliminary scout images were acquired on sagittal and coronal planes for slice positioning. Coronal T2-weighted images were acquired to enable visualization of orthotopic colon tumors. Data acquisition consisted of a localizer, T1-weighted MR images, and T2-weighted MR images. Anatomic coverage included the tumor, kidneys, and muscles. T1-weighted dynamic contrast-enhanced MRI (DCE-MRI) was performed using the intravascular contrast agent, albumin-gadopentetate dimeglumine (albumin-GdDTPA; University of California, San Francisco, CA, USA) (13). T1-relaxation rate measurements were performed using a saturation recovery, fast spin echo (FSE) sequence with an effective echo time of 10 ms, and a TR ranging from 360 to 6000 milliseconds [FOV=32×32 mm, slice thickness=1.0 mm, matrix size=128×96 pixels, number of excitations (NEX)=3. RARE factor=8]. Three coronal T1-FSE scans were acquired before contrast and five T1-FSE scans were acquired after administration of albumin-GdDTPA (0.1 mmol/kg). Image processing and analysis were carried out using commercially available software (ANALYZE PC, Version 7.0; Biomedical Imaging Resource, Mayo Foundation, Rochester, MN, USA) (Matlab's curve-fitting toolbox, Matlab Version 7.0; Math Works, Inc., Natick, MA, USA). Relative blood volume was calculated by linear regression analysis of the normalized change in T1-relaxation rate ($\Delta R1_{tumor/blood}$) of tumors as described by us previously (8, 13). Kidneys were sampled and used as a surrogate measure of the contrast agent concentration in the blood.

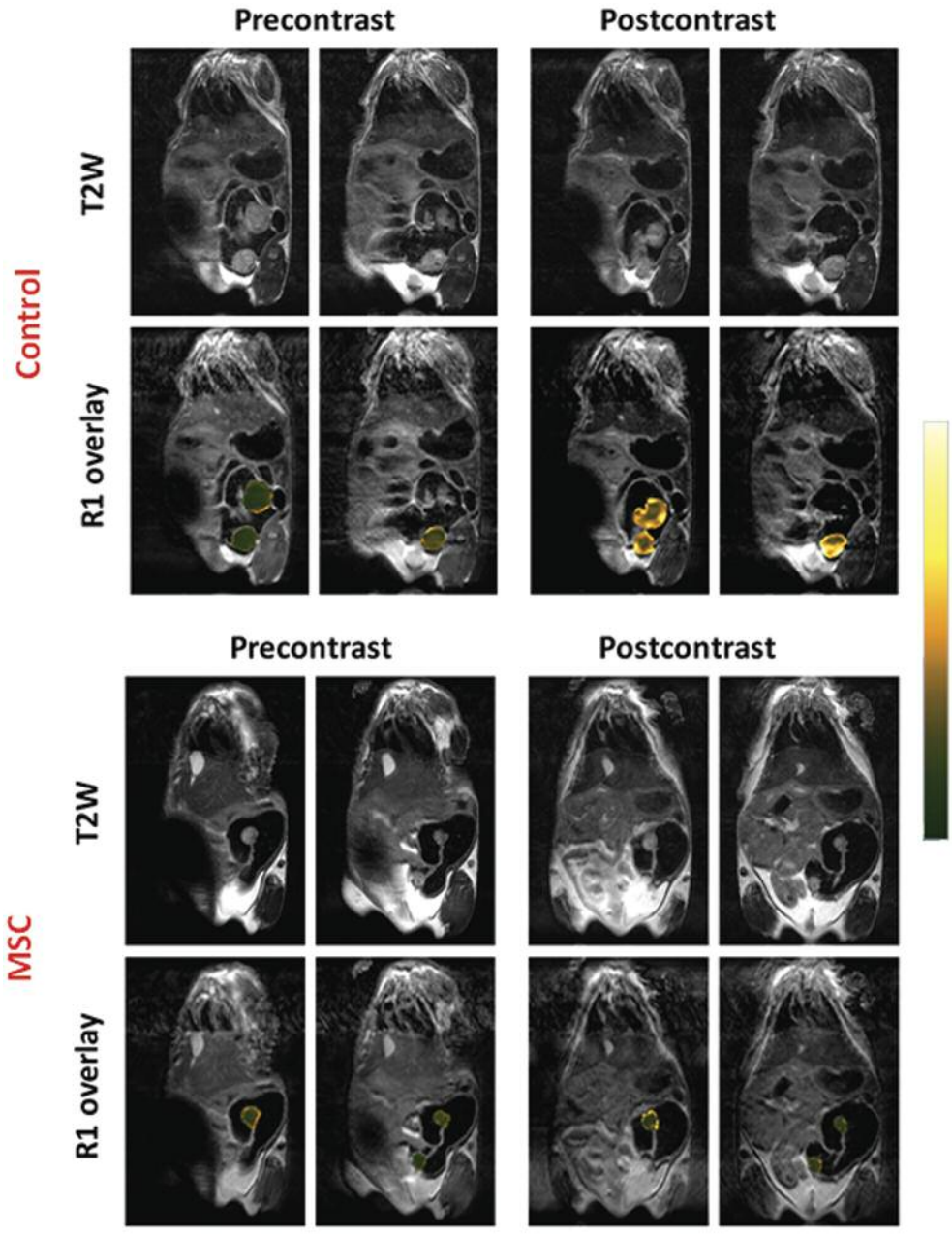

Figure 2. *DCE-MRI of vascular response to selenium. Panel of images shown in the figure represent T2-weighted MR images (T2W) and corresponding R1 maps of a control animal and a selenium-treated animal before (pre-contrast) and after (post-contrast) administration of albumin-GdDTPA. Pseudocolorized images of the tumors overlaid on top of the raw proton images of two contiguous slices are shown along with the corresponding T2-weighted images for visualization of tumor. Control tumors exhibited a marked degree of T1-enhancement following administration of albumin-GdDTPA compared to precontrast images, indicative of the presence of a functioning vascular network. In contrast, post-contrast R1 maps of GEO tumors in MSC-treated animals showed minimal enhancement compared to pre-contrast images, suggestive of reduction in functional vasculature following selenium treatment.*

Immunohistochemistry. CD31 immunostaining of untreated controls and MSC-treated tumors (0.2 mg/day × 14) was performed using previously described methods (8, 9). All CD31-positive intratumor microvessels were counted at ×400 magnification in each individual microscopic field on the viable parts of the entire tumor without any selection criteria. Single CD31-positive endothelial cells without any visible lumen were not counted. The results were reported as the average MVD per high-power field.

Statistical analysis. Measured values are reported as mean±standard error of the mean. MRI/FPI studies were performed using a total of

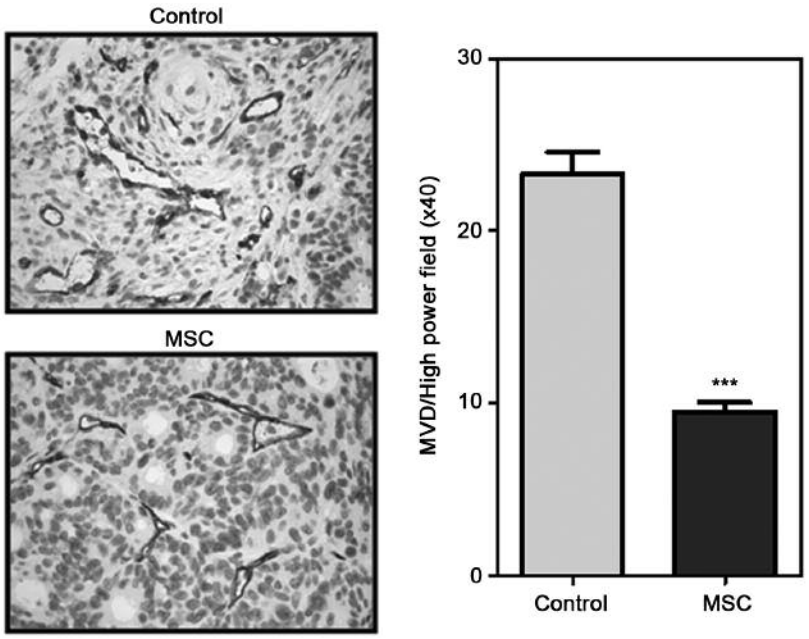

Figure 3. *Immunohistochemical staining of microvessel density (MVD) in GEO tumors following selenium treatment. Representative photomicrographs of CD31-immunostained GEO tumor sections obtained from a control animal and an animal treated with 0.2 mg/kg MSC for 14 days are shown. As shown in the bar graph on the right, treatment with MSC led to a significant reduction in MVD (p<0.001).*

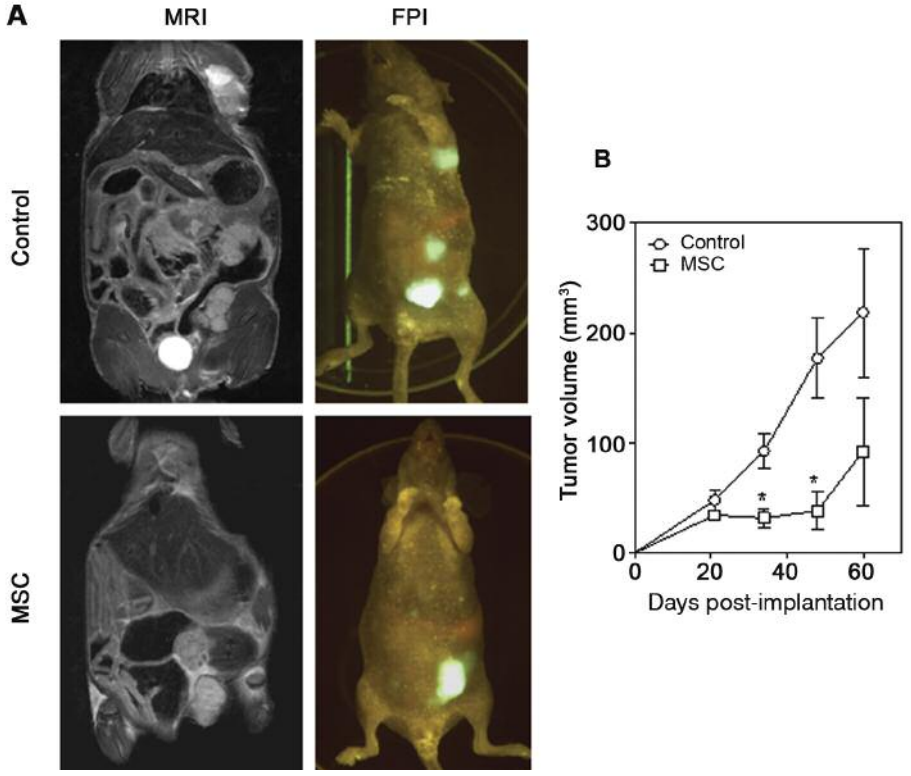

Figure 4. *Combined MRI-GFP FPI of GEO tumor response to selenium. The antitumor activity of selenium against orthotopic GEO tumors was examined by monitoring tumor growth over a 60-day period using combined MRI and FPI. (A) Coronal T2-weighted MR images of a control mouse and a selenium-treated mouse on day 60 post-implantation are shown on the left. Corresponding FPI (GFP) images of an animal from each group are also shown on the right. (B) Plot shows the change in volumes of control (n=6) and selenium-treated tumors (n=5) at different times post-implantation. Significant differences in tumor volume were seen on days 34 and 48 following implantation (p=0.01).*

eleven tumors (six controls, five MSC) in eight animals. DCE-MRI studies were performed on a total of sixteen tumors (eight controls, eight MSC) in eight animals. However, data from one MSC-treated animal (m5) were excluded from the analysis due to a poor contrast-agent injection evidenced by lack of enhancement in the kidneys post-contrast. DCE-MRI data analysis was therefore performed using eight control tumors and six MSC-treated tumors. Immunohistochemical analysis was also performed on sixteen tumors (eight controls, eight MSC). Animals that did not reveal successful tumor 'take' were excluded from the study. A two-tailed Student's *t*-test was used for comparing treatment groups with untreated controls. *P*-values less than 0.05 were considered statistically significant. All statistical calculations and analyses were performed using Graph Pad Prism (Version 5.00; Graph Pad, San Diego, CA, USA).

Results

The progress of orthotopic colon tumors was visualized in nude mice using MRI and FPI. Serial FPI was performed once every three to four days beginning one week post-implantation. MRI was performed once a week. Whole-body FPI provided evidence of tumor growth seven days after surgical implantation even in the absence of a palpable tumor. As shown in Figure 1, both MRI and FPI enabled excellent tumor localization. T1- and T2-weighted MRI provided adequate contrast and volumetric assessment of GEO tumor growth. FPI allowed for high-throughput screening of tumor growth at different times post-implantation.

In addition to anatomic imaging of tumor growth using MRI and FPI, the effects of selenium therapy on the vascularization of GEO colon tumors were assessed. To accomplish this, DCE-MRI was performed using an intravascular contrast agent, albumin-Gd-DTPA. DCE-MRI was performed on a total of eight animals (four control, four MSC) following daily treatment with selenium for a period of 17 days beginning day six after implantation. This time point was chosen based on the antiangiogenic efficacy of selenium observed in our previous studies using subcutaneous human tumor xenograft models (8, 9).

Figure 2 shows T1-relaxation maps (R1=1/T1) of a control animal and an MSC-treated animal before (pre-contrast) and after (post-contrast) administration of albumin-GdDTPA. Pseudocolorized images of the tumors overlaid on top of the raw proton images of two contiguous slices are shown along with the corresponding T2-weighted images for visualization of tumor. Control tumors exhibited a marked degree of T1-enhancement following administration of albumin-GdDTPA compared to precontrast images, indicative of the presence of a functioning vascular network. In contrast, post-contrast R1 maps of GEO tumors in selenium-treated animals showed minimal enhancement compared to pre-contrast images, suggestive of decreased tumor vascularization. The relative blood volume of tumors was calculated from the change in T1-relaxation rate (ΔR1) following contrast. Linear regression analysis of the normalized $\Delta R1_{(tumor/blood)}$ over the 40 minute post-contrast imaging period revealed a significant (p=0.007) reduction in blood volume of MSC-treated tumors (0.085±0.04) compared to untreated controls (0.12±0.01).

To validate the findings obtained with MRI on the efficacy of selenium treatment on GEO vascular function, orthotopic GEO tumor-bearing mice were treated with MSC for a period of 14 days beginning 6 days after implantation. Tumors were excised and immunostained for CD31. Tumor sections obtained from control animals appeared to be well vascularized with an average MVD of 23.30±1.2 (n=8). Treatment with MSC led to a significant reduction in MVD (p<0.001; 9.50±0.5, n=8). Representative images of CD31-immunostained GEO tumor sections obtained from a control animal and an animal treated with 0.2 mg/kg MSC for 14 days are shown in Figure 3.

The antitumor efficacy of selenium treatment was examined by monitoring tumor growth over a 60-day period using combined MRI and FPI. Coronal T2-weighted MR images of a control mouse and an MSC-treated mouse on day 60 are shown in Figure 4A. Corresponding FPI (GFP) images of an animal from each group are also shown. Figure 4B depicts the change in volumes of control (n=6) and MSC-treated tumors (n=5) at different times post-implantation. Tumor volume was calculated from multislice T2-weighted MR images acquired on the coronal plane. No significant difference in tumor volume was observed between animals in the control and MSC treatment groups on day 21 (control 47.95±9.5 mm^3; MSC 34.26±4.0 mm^3, p=0.252). However, extended treatment with MSC resulted in a significant reduction in tumor growth compared to untreated controls on day 34 (92.49±15.7 mm^3 *vs*. 31.64±8.9 mm^3, p=0.011) and on day 48 (177.0±36.4 mm^3 *vs*. 38.29±17 mm^3, p=0.0106). MSC-treated tumors showed a delay in tumor regrowth during the 60-day monitoring period. However, differences in tumor volumes of controls (218.46±58.3 mm^3) and selenium-treated animals (92.15±49.0 mm^3) at day 60 were not statistically significant (p=0.1407).

Discussion

Colorectal cancer is one of the leading causes of cancer-related mortality in the United States (14). Given its biologic complexity and poor prognosis, it is important to evaluate novel treatment strategies that might potentially improve treatment outcome in patients. The essential dietary trace element, selenium, has been shown to act as an effective chemopreventive agent reducing the risk and mortality associated with cancer (15, 16). MSC is an organoselenium compound that has been shown to exert potent antiangiogenic activity *in vivo* (8, 9, 17, 18). The antiangiogenic effects of selenium have previously been demonstrated in ectopic subcutaneous models of human head and neck, colorectal and lung cancer (8, 9).

Monitoring of subcutaneous (ectopic) tumors in small animals can be performed easily through the combination of visual inspection and simple caliper-based measurements of tumor dimension. In contrast, tumors established in orthotopic tumor sites cannot be assessed by visual examination and are often palpable only during advanced stages of tumor growth.

It is widely recognized that orthotopic tumor models provide an appropriate simulation of the local tumor tissue microenvironment and are therefore better suited for preclinical evaluation of therapeutics (12, 19). In this regard, optical imaging techniques such as FPI provide advantages over methods such as MRI and CT, and enable high-throughput imaging of small animals in an economically feasible manner (20). MRI and FPI have previously been compared for the assessment of orthotopic pancreatic tumors in mice (6). The results of that previous study revealed a strong correlation between three-dimensional MRI-based measurements of tumor volume and FPI-based measurements of tumor area in an orthotopic model of pancreatic cancer. Recently, Gros *et al*. highlighted the utility of combined MRI and FPI in an orthotopic metastatic model of esophageal cancer (7).

Such multimodality imaging approaches have the potential to provide useful insight into the biology of orthotopic tumors and facilitate validation of tumor response to therapy. Therefore, in the present study, a dual-modality imaging approach was implemented using FPI and MRI to demonstrate the antiangiogenic and antitumor activity of selenium in an orthotopic model of human colon cancer in nude mice. Both FPI and MRI provided evidence of the therapeutic activity against the GEO colon adenocarcinomas. While whole-body FPI enabled high-throughput longitudinal monitoring of tumor growth and progression, MRI facilitated the quantification of vascular changes in the orthotopic colon tumors following therapeutic intervention. The complimentary nature of MRI and FPI allowed for simultaneous determination of tumor progression and angiogenesis and their response to therapy.

MRI methods have been widely utilized in both preclinical and clinical settings for assessment of tumor response to therapy. Although FPI requires gene transfection of tumor cells which is currently not available clinically (21), fluorescence imaging techniques are being pursued for diagnostic clinical applications in oncology including early detection of neoplastic disease and mapping of sentinel lymph nodes with encouraging results (22, 23).

In previous studies using subcutaneous tumors, the antiangiogenic efficacy of selenium has been observed consistently, particularly in well-vascularized, poorly differentiated tumors (9). Using immunohistochemistry, increased tumor vascular maturation following selenium treatment has also been demonstrated (8). The current study demonstrates the anti-angiogenic and antitumor activity of MSC in a clinically-relevant model. A significant decrease in MVD of orthotopic GEO colon tumors (Figure 3A) was observed with MSC treatment. This is consistent with a previous study in subcutaneous colon tumors in which a reduction in MVD and lowering of tumor interstitial fluid pressure with MSC treatment was observed. This resulted in higher intratumor drug delivery and, subsequently, a higher therapeutic response in combination with chemotherapy (9).

In the clinical setting, blocking VEGF alone (*e.g.* with bevacizumab) has met with limited therapeutic success in solid tumors, including colorectal cancer (24). In glioblastomas, an infiltrative phenotype with increased local invasion and distant metastasis has been observed after withdrawal of VEGF blockade (25). It was previously demonstrated that the antiangiogenic and chemomodulatory activity of MSC is mediated by down-regulation of VEGF, Cox-2, HIF-1α and iNOS (26). Recently, it was also demonstrated that MSC sensitizes hypoxic tumor cells to chemotherapy by targeting HIF-1α (27). The ability of MSC to block multiple regulators of angiogenesis might therefore lead to more effective and sustained angiogenic inhibition compared to agents targeted towards a single angiogenic molecule.

In conclusion, the results of this study highlight the usefulness of multimodal imaging approaches in the assessment of tumor and angiogenic response to therapy and demonstrate the antiangiogenic effects of selenium in an orthotopic model of human colon cancer. However, a few limitations of the study need to be recognized. Although both MRI and FPI were used to monitor tumor progression and therapeutic response, only qualitative (visual) comparisons were made between the two imaging methods. However, previous studies have demonstrated good correlation between quantitative measurements of tumor volume and area obtained using MRI and FPI, respectively (6, 7). Secondly, the effects of selenium treatment on colorectal liver metastases were not investigated. Further investigation is therefore warranted to evaluate the benefits of selenium therapy particularly in combination with chemotherapy in control of primary and metastatic colorectal cancer.

Acknowledgements

This research was supported by grants from the National Cancer Institute (NCI) 1R21 CA133682-01A2 (A.B.), Alliance Foundation (M.S) and utilized core resources supported by RPCI's Comprehensive Cancer Center Support Grant CA016056 from the NCI.

References

1 Tentler JJ, Bradshaw-Pierce EL, Serkova NJ, Hasebroock KM, Pitts TM, Diamond JR, Fletcher GC, Bray MR and Eckhardt SG: Assessment of the *in vivo* antitumor effects of ENMD-2076, a novel multitargeted kinase inhibitor, against primary and cell line-derived human colorectal cancer xenograft models. Clin Cancer Res *16(11)*: 2989-2998, 2010.

2 Sabir A, Schor-Bardach R, Wilcox CJ, Rahmanuddin S, Atkins MB, Kruskal JB, Signoretti S, Raptopoulos VD and Goldberg SN: Perfusion MDCT enables early detection of therapeutic response to antiangiogenic therapy. Am J Roentgenol *191(1)*: 133-139, 2008.
3 Finnberg N, Kim SH, Furth EE, Liu JJ, Russo P, Piccoli DA, Grimberg A and El-Deiry WS: Non-invasive fluorescence imaging of cell death in fresh human colon epithelia treated with 5-Fluorouracil, CPT-11 and/or TRAIL. Cancer Biol Ther *4(9)*: 937-942, 2005.
4 Deroose CM, De A, Loening AM, Chow PL, Ray P, Chatziioannou AF and Gambhir SS: Multimodality imaging of tumor xenografts and metastases in mice with combined small-animal PET, small-animal CT, and bioluminescence imaging. J Nucl Med *48(2)*: 295-303, 2007.
5 Zhao D, Richer E, Antich PP and Mason RP: Antivascular effects of combretastatin A4 phosphate in breast cancer xenograft assessed using dynamic bioluminescence imaging and confirmed by MRI. FASEB J *22(7)*: 2445-2451, 2008.
6 Bouvet M, Spernyak J, Katz MH, Mazurchuk RV, Takimoto S, Bernacki R, Rustum YM, Moossa AR and Hoffman RM: High correlation of whole-body red fluorescent protein imaging and magnetic resonance imaging on an orthotopic model of pancreatic cancer. Cancer Res *65(21)*: 9829-9833, 2005.
7 Gros SJ, Dohrmann T, Peldschus K, Schurr PG, Kaifi JT, Kalinina T, Reichelt U, Mann O, Strate TG, Adam G, Hoffman RM and Izbicki JR: Complementary use of fluorescence and magnetic resonance imaging of metastatic esophageal cancer in a novel orthotopic mouse model. Int J Cancer *126(11)*: 2671-2681, 2010.
8 Bhattacharya A, Seshadri M, Oven SD, Tóth K, Vaughan MM and Rustum YM: Tumor vascular maturation and improved drug delivery induced by methylselenocysteine leads to therapeutic synergy with anticancer drugs. Clin Cancer Res *14(12)*: 3926-3932, 2008.
9 Bhattacharya A, Tóth K, Sen A, Seshadri M, Cao S, Durrani FA, Faber E, Repasky EA and Rustum YM: Inhibition of colon cancer growth by methylselenocysteine-induced angiogenic chemomodulation is influenced by histologic characteristics of the tumor. Clin Colorectal Cancer *8(3)*: 155-162, 2009.
10 Rajput A, Dominguez San Martin I, Rose R, Beko A, Levea C, Sharratt E, Mazurchuk R, Hoffman RM, Brattain MG and Wang J: Characterization of HCT116 human colon cancer cells in an orthotopic model. J Surg Res *147(2)*: 276-281, 2008.
11 Rose RJ, Wang J, Hu P, Le Vea C, Brattain MG and Rajput A: Characterization of the GEO human colon cancer cell line in an orthotopic model of colon cancer. J Surg Res *130(2)*: 258, 2006.
12 Hoffman RM: Orthotopic metastatic mouse models for anticancer drug discovery and evaluation: a bridge to the clinic. Investigational New Drugs *17*: 343-359, 1999.
13 Seshadri M, Mazurchuk R, Spernyak JA, Bhattacharya A, Rustum YM and Bellnier DA: Activity of the vascular-disrupting agent 5,6-dimethylxanthenone-4-acetic acid against human head and neck carcinoma xenografts. Neoplasia *8(7)*: 534-542, 2006.
14 Jemal A, Siegel R, Xu J and Ward E: Cancer statistics, 2010. CA Cancer J Clin *60(5)*: 277-300, 2010.
15 Clark LC, Combs GF Jr., Turnbull BW, Slate EH, Chalker DK, Chow J, Davis LS, Glover RA, Graham GF, Gross EG, Krongrad A, Lesher JL Jr., Park HK, Sanders BB Jr., Smith CL and Taylor JR: Effects of selenium supplementation for cancer prevention inpatients with carcinoma of the skin. A randomized controlled trial. Nutritional Prevention of Cancer Study Group. J Am Med Assoc *276*: 1957-1963, 1996.
16 Duffield-Lillico AJ, Slate EH, Reid ME, Turnbull BW, Wilkins PA, Combs GF Jr., Park HK, Gross EG, Graham GF, Stratton MS, Marshall JR and Clark LC: Nutritional Prevention of Cancer Study Group: Selenium supplementation and secondary prevention of nonmelanoma skin cancer in a randomized trial. J Natl Cancer Inst *95*: 1477-1481, 2003.
17 Jiang C, Jiang W, Ip C and Lu J: Selenium-induced inhibition of angiogenesis in mammary cancer at chemopreventive levels of intake. Mol Carcinog *26*: 213-225, 1999.
18 Jiang C, Ganther H and Lu J: Monomethyl selenium-specific inhibition of MMP-2 and VEGF expression: implications for angiogenic switch regulation. Mol Carcinog 29: 236-250, 2000.
19 Fidler IJ, Kim SJ and Langley RR: The role of the organ microenvironment in the biology and therapy of cancer metastasis. J Cell Biochem *101(4)*: 927-936, 2007.
20 Hoffman RM: The multiple uses of fluorescent proteins to visualize cancer *in vivo*. Nat Rev Cancer *5*: 796-806, 2005.
21 Kishimoto H, Zhao M, Hayashi K, Urata Y, Tanaka N, Fujiwara T, Perman S and Hoffman RM: *In vivo* internal tumor illumination by telomerase-dependent adenoviral GFP for precise surgical navigation. Proc Natl Acad Sci USA *106*: 14514-14517, 2009.
22 Crane LM, Themelis G, Buddingh T, Harlaar NJ, Pleijhuis RG, Sarantopoulos A, van der Zee AG, Ntziachristos V and van Dam GM: Multispectral real-time fluorescence imaging for intraoperative detection of the sentinel lymph node in gynecologic oncology. J Vis Exp 44:. pii: 2225, 2010. doi: 10.3791/2225.
23 Tagaya N, Aoyagi H, Nakagawa A, Abe A, Iwasaki Y, Tachibana M and Kubota K: A novel approach for sentinel lymph node identification using fluorescence imaging and image overlay navigation surgery in patients with breast cancer. World J Surg *35(1)*: 154-158, 2011.
24 Hubbard J and Grothey A: Antiangiogenesis agents in colorectal cancer. Curr Opin Oncol *22(4)*: 374-380, 2010.
25 de Groot JF, Fuller G, Kumar AJ, Piao Y, Eterovic K, Ji Y and Conrad CA: Tumor invasion after treatment of glioblastoma with bevacizumab: radiographic and pathologic correlation in humans and mice. Neuro Oncol *12(3)*: 233-242, 2010.
26 Yin MB, Li ZR, Tóth K, Cao S, Durrani FA, Hapke G, Bhattacharya A, Azrak RG, Frank C and Rustum YM: Potentiation of irinotecan sensitivity by Se-methylselenocysteine in an *in vivo* tumor model is associated with down-regulation of cyclooxygenase-2, inducible nitric oxide synthase, and hypoxia-inducible factor 1alpha expression, resulting in reduced angiogenesis. Oncogene *25(17)*: 2509-2519, 2006.
27 Chintala S, Tóth K, Cao S, Durrani FA, Vaughan MM, Jensen RL and Rustum YM: Se-methylselenocysteine sensitizes hypoxic tumor cells to irinotecan by targeting hypoxia-inducible factor 1alpha.Cancer Chemother Pharmacol *66(5)*: 899-911, 2010.

Received December 29, 2010
Revised January 24, 2011
Accepted January 25, 2011